Multi-Domain Quantitative ECG Analysis Reveals Distinct Morphological Patterns in Brugada Syndrome

Ziyu Li[1], Dillon J Dzikowicz[2], Ben Bailey[2], Michael Silka[3], Junmo An[2]

[1]Philips, Eindhoven, Netherlands
[2]Philips, Cambridge, MA, USA
[3]Children's Hospital Los Angeles, Los Angeles, California, USA

Abstract

Brugada syndrome is associated with an increased risk of sudden cardiac death and is diagnosed primarily by visual assessment of ECG morphology in the right precordial leads. We evaluated whether automated quantitative ECG measurements could characterize the Brugada phenotype beyond conventional visual criteria. Standard 12-lead ECG recordings from the Brugada-HUCA database were analyzed, including 69 participants with Brugada syndrome and 287 controls. Automated measurements from representative beats were compared in leads V1 and V2 using Mann-Whitney rank-sum tests. Brugada syndrome was associated with higher STJ amplitude and more negative ST-segment slope in both leads. The J-Tpeak interval was significantly shorter in the Brugada group, whereas ST-segment duration did not differ significantly between groups. QRS area and T-wave area also differed significantly in both leads. Representative-beat analysis localized the principal morphological differences to the J-point, ST segment, and T-wave regions. These findings provide interpretable quantitative markers of the Brugada ECG phenotype that may complement visual ECG assessment and support future automated detection approaches.

1. Introduction

Brugada syndrome is a heritable arrhythmia syndrome associated with ventricular fibrillation and sudden cardiac death in the absence of overt structural heart disease [1]. It is more prevalent among men and particularly common in Southeast Asia [2]. Its hallmark type 1 ECG pattern, characterized by coved ST-segment elevation ≥ 0.2 mV in at least one right precordial lead, V1 or V2, followed by T-wave inversion, may be intermittent and can be unmasked by fever, sodium-channel-blocking agents, or changes in autonomic tone [3].

Conventional diagnosis relies primarily on visual recognition of this ECG pattern by trained clinicians and may therefore be affected by reader-dependent interpretation, particularly when the phenotype is borderline or intermittent. Traditional computerized ECG interpretation uses predefined waveform measurements and diagnostic criteria. Although these systems can support clinical interpretation, limitations in diagnostic accuracy remain, and expert over-reading is required [4]. Such approaches may not fully quantify the broader morphological abnormalities present across the 12-lead ECG.

A more comprehensive quantitative characterization of ECG morphology may therefore complement visual interpretation and rule-based assessment. The right precordial leads V1 and V2 are central to the Brugada phenotype because they capture its characteristic ST-segment and repolarization abnormalities. Recent work has also shown that explainable deep learning applied to 12-lead ECGs can support automated Brugada detection [5].

This study aimed to characterize the quantitative ECG signature of Brugada syndrome using automated measurements across four feature domains: amplitude, slope, duration, and area. We focused on leads V1 and V2 and compared group-average representative beats to examine morphological differences across the J-point, ST-segment, and T-wave regions.

2. Methods

2.1. Dataset

The Brugada-HUCA database (version 1.0.0), a publicly available and de-identified dataset hosted on PhysioNet, was used in this study [6]. The database contains 363 standard 12-lead ECG recordings obtained from individuals evaluated for suspected Brugada syndrome at the Hospital Universitario Central de Asturias. Each waveform record is linked to a single metadata entry and includes leads I, II, III, aVR, aVL, aVF, and V1-V6. Recordings were acquired for 12 seconds at a sampling frequency of 100 Hz, and signal amplitudes were

provided in millivolts.

The diagnostic variable in the accompanying metadata classified recordings as controls (code 0), confirmed Brugada syndrome cases (code 1), or other/atypical cases (code 2). The dataset included 287 controls, 69 confirmed Brugada cases, and 7 other/atypical cases.

2.2. Preprocessing and Study Cohort

For the primary analysis, recordings labelled as other/atypical cases (code 2) were excluded, yielding an analytic cohort of 69 participants with Brugada syndrome and 287 controls. Each 12-second ECG recording was shortened to a 10-second segment and resampled from 100 Hz to 500 Hz using finite impulse response (FIR)-based band-limited interpolation. The resulting recordings contained 5,000 samples for each of the 12 ECG leads. The 10-second, 12-lead ECG recordings sampled at 500 Hz were used as input for representative-beat generation and automated quantitative measurement. The preprocessing procedure was applied identically to all recordings.

2.3. Feature Extraction

Automated ECG analysis was performed using the Philips DXL algorithm. The algorithm detected and extracted beat complexes from each recording, grouped them according to rate and morphology, and excluded outlier complexes. The remaining beats within the dominant beat family were averaged to generate a 1.2-second representative beat sampled at 1,000 Hz for each ECG lead. These representative beats were used for automated measurement extraction and group-level waveform comparisons.

The Philips DXL algorithm provides a wide range of global and lead-specific ECG measurements. In this study, we analyzed a prespecified subset of lead-specific measurements in leads V1 and V2, including ST-junction (STJ) amplitude, ST-segment slope, J-Tpeak duration, ST-segment duration, QRS area, and T-wave area.

2.4. Statistical Analysis

Quantitative ECG features were compared between the Brugada and control groups using two-sided Mann-Whitney rank-sum tests. Missing values were excluded on a feature-specific basis. A p-value < 0.05 was considered statistically significant.

Continuous variables are presented as median and interquartile range (IQR). For visualization, individual measurements were displayed using box plots, with black diamonds indicating group means. Group-average representative beats were calculated at each time point and displayed as means with shaded standard error of the mean (SEM) bands. Statistical analyses were performed using MATLAB (version R2021a, MathWorks, Natick, MA, USA).

3. Results

3.1. Representative-beat morphology in Brugada syndrome and controls

DXL-derived representative beats were averaged within each group, and the SEM was calculated at each sample point. Average representative beats differed between the Brugada and control groups in V1 and V2, mainly around the J-point, ST segment, and T wave. In V1, the Brugada group showed greater J-point elevation, a more pronounced downsloping ST segment, and more negative T-wave deflection. Similar differences were observed in V2, with greater ST-segment elevation and altered T-wave morphology (Figure 1).

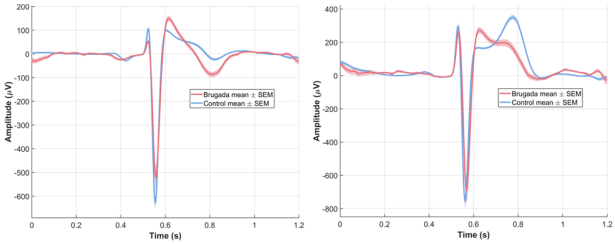

Figure 1. Group-average DXL-derived representative beats in V1 and V2 for Brugada syndrome (red) and controls (blue). Shading indicates SEM.

3.2. STJ Amplitude

STJ amplitude was significantly higher in the Brugada group than in the control group in both V1 and V2 (Figure 2). In V1, median STJ amplitude was 141.0 μV (IQR, 109.8-210.5 μV) in the Brugada group, compared with 98.0 μV (IQR, 58.3-139.8 μV) in the control group (Mann-Whitney rank-sum $p < 0.0001$). In V2, median STJ amplitude was 308.0 μV (IQR, 225.8-426.5 μV) in the Brugada group and 171.0 μV (IQR, 107.0-248.5 μV) in the control group ($p < 0.0001$). The between-group difference was more pronounced in V2, consistent with the characteristic right precordial J-point elevation associated with the Brugada ECG phenotype.

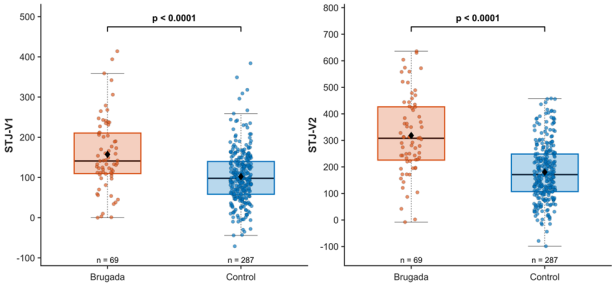

Figure 2. STJ amplitude in V1 (left) and V2 (right) for Brugada syndrome (red) and controls (blue). Black diamonds indicate means; $p < 0.0001$ by Mann-Whitney rank-sum test.

3.3. ST-Segment Slope

ST-segment slope was more negative in the Brugada group than in the control group in both V1 and V2 (Figure 3). In V1, the median slope was -26.0 µV/ms (IQR, -37.0 to -18.0 µV/ms) in the Brugada group, compared with -9.0 µV/ms (IQR, -17.0 to -2.0 µV/ms) in the control group (Mann-Whitney rank-sum $p < 0.0001$). In V2, the median slope was -28.0 µV/ms (IQR, -39.3 to -10.0 µV/ms) in the Brugada group and 4.0 µV/ms (IQR, -7.0 to 20.0 µV/ms) in the control group ($p < 0.0001$). These findings indicate a more pronounced downsloping ST-segment morphology in Brugada syndrome.

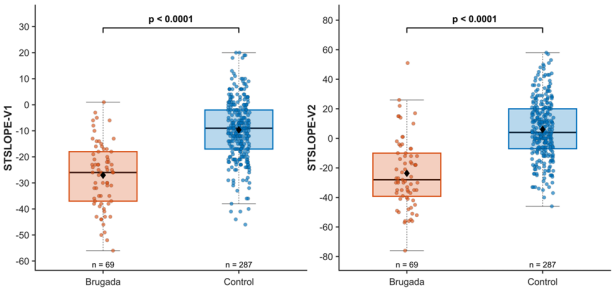

Figure 3. ST-segment slope in V1 (left) and V2 (right) for Brugada syndrome (red) and controls (blue). Black diamonds indicate means; $p < 0.0001$ by Mann-Whitney rank-sum test.

3.4. J-Tpeak and ST-Segment Durations

The J-Tpeak interval was shorter in the Brugada group than in controls in both V1 and V2 (Figure 4). In V1, the median J-Tpeak interval was 158.0 ms (IQR, 143.0-176.3 ms) in the Brugada group and 175.5 ms (IQR, 149.0-205.5 ms) in controls (Mann-Whitney rank-sum $p < 0.01$). In V2, the median interval was 150.5 ms (IQR, 105.0-181.0 ms) in the Brugada group and 172.0 ms (IQR, 150.0-193.3 ms) in controls ($p < 0.01$). In contrast, ST-segment duration did not differ significantly between the Brugada and control groups in either V1 or V2 (both $p > 0.05$; data not shown).

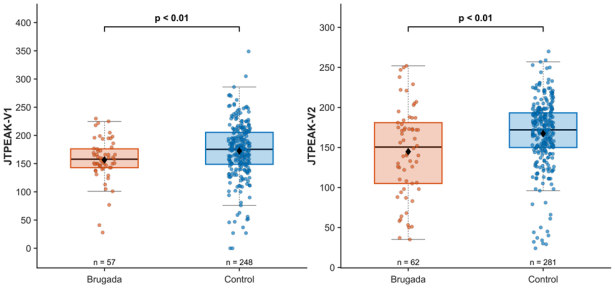

Figure 4. J-Tpeak interval in V1 (left) and V2 (right) for Brugada syndrome (red) and controls (blue). Black diamonds indicate means; $p < 0.01$ by Mann-Whitney rank-sum test.

3.5. QRS and T Areas

QRS area was less negative in the Brugada group than in controls in both V1 and V2 (Figure 5). In V1, the median QRS area was -23.0 µV·ms (IQR, -41.3 to -2.8 µV·ms) in the Brugada group and -32.0 µV·ms (IQR, -54.0 to -15.0 µV·ms) in controls (Mann-Whitney rank-sum $p < 0.01$). In V2, the median QRS area was 7.0 µV·ms (IQR, -46.3 to 38.3 µV·ms) in the Brugada group and -24.0 µV·ms (IQR, -56.0 to 2.8 µV·ms) in controls ($p < 0.01$).

T-wave area also differed between groups in both leads (Figure 6). In V1, the median T-wave area was -20.0 µV·ms (IQR, -37.5 to 1.0 µV·ms) in the Brugada group and 1.0 µV·ms (IQR, -19.0 to 22.5 µV·ms) in controls ($p < 0.0001$). In V2, the median T-wave area was 33.0 µV·ms (IQR, -14.0 to 83.3 µV·ms) in the Brugada group and 102.0 µV·ms (IQR, 53.3 to 168.0 µV·ms) in controls ($p < 0.0001$).

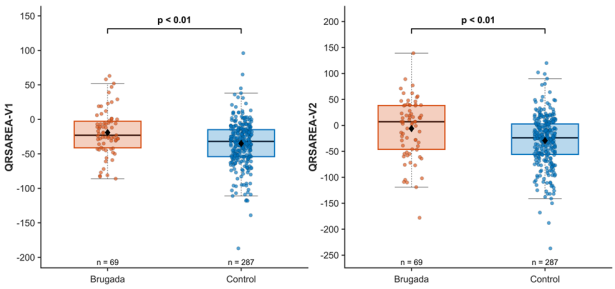

Figure 5. QRS area in V1 (left) and V2 (right) for Brugada syndrome (red) and controls (blue). Black diamonds indicate means; $p < 0.01$ by Mann-Whitney rank-sum test.

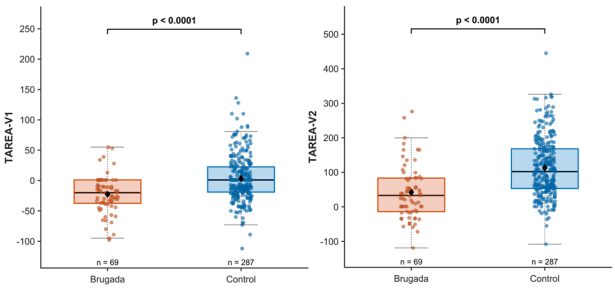

Figure 6. T-wave area in V1 (left) and V2 (right) for Brugada syndrome (red) and controls (blue). Black diamonds indicate means; $p < 0.0001$ by Mann-Whitney rank-sum test.

4. Discussion

This study identified consistent quantitative differences in representative-beat morphology between participants with Brugada syndrome and controls in the right precordial leads. The observed group differences were concentrated around the J-point, ST segment, and T wave, corresponding to the principal morphological components

of the type 1 Brugada ECG pattern. These findings support the value of automated quantitative measurements as complementary tools for characterizing abnormalities that are typically evaluated by visual ECG interpretation.

STJ amplitude was significantly higher in the Brugada group in both V1 and V2. This finding quantitatively captures the J-point elevation that is central to the Brugada ECG phenotype. ST-segment slope was also substantially more negative in the Brugada group in both leads, indicating a more pronounced downsloping ST-segment contour. Taken together, elevated STJ amplitude and a negative ST-segment slope provide complementary measurements of the coved morphology: the former reflects the magnitude of initial ST elevation, whereas the latter reflects its subsequent decline.

The J-Tpeak interval was shorter in the Brugada group in both V1 and V2, suggesting altered timing of early ventricular repolarization. In contrast, ST-segment duration did not differ significantly between groups. This pattern indicates that group separation was more evident in ST-segment configuration, including amplitude and slope, than in overall ST-segment duration. Thus, quantitative assessment of waveform shape may be more informative than duration alone for characterizing the Brugada ECG phenotype.

Area-based measurements further demonstrated differences in depolarization and repolarization morphology. QRS area was less negative in the Brugada group in both V1 and V2, indicating altered integrated QRS morphology in the right precordial leads. T-wave area was more negative in V1 and lower in V2 in the Brugada group, consistent with the altered T-wave morphology observed in the representative beats. These findings may be compatible with abnormal ventricular depolarization and repolarization in Brugada syndrome; however, surface ECG measurements alone cannot establish the underlying electrophysiological mechanism.

The present findings have potential relevance for automated ECG analysis. Rather than relying solely on fixed ST-elevation thresholds, automated systems could incorporate complementary waveform measurements, including STJ amplitude, ST-segment slope, J-Tpeak duration, and QRS and T-wave areas. Such structured features may also complement deep learning approaches by providing clinically interpretable measurements for model development and explainability analyses [5]. Their value for diagnostic classification, phenotype severity assessment, and risk stratification requires independent validation.

This study has several limitations. First, the analysis used a single-center public dataset with an imbalanced number of Brugada and control recordings and without matching for demographic or clinical characteristics. Second, Brugada ECG patterns are dynamic, whereas each participant contributed a single short-duration ECG recording. Third, the measurements were derived using the proprietary Philips DXL algorithm; therefore, their reproducibility across alternative ECG-analysis platforms should be assessed. Fourth, feature-wise statistical testing was performed without multiple-comparison correction, and findings beyond the primary features should be interpreted cautiously. Finally, this study compared Brugada syndrome with controls only and did not evaluate clinically relevant ECG mimics, including right bundle branch block, early repolarization, or Brugada phenocopies.

Future work should validate these measurements in independent multicenter cohorts, assess their robustness across ECG acquisition conditions and analysis platforms, and compare Brugada syndrome with clinically relevant mimics. Integrating structured quantitative features with explainable deep learning models may help improve automated Brugada detection while preserving clinically interpretable outputs. Prospective studies incorporating clinical outcomes will also be needed to determine whether these ECG measurements provide prognostic information beyond diagnostic classification.

References

[1] C. Antzelevitch *et al.*, "Brugada syndrome: report of the second consensus conference: endorsed by the Heart Rhythm Society and the European Heart Rhythm Association," *Circulation*, vol. 111, no. 5, pp. 659–670, 2005.

[2] W. Vutthikraivit *et al.*, "Worldwide prevalence of Brugada syndrome: a systematic review and meta-analysis," *Acta Cardiol. Sin.*, vol. 34, no. 3, p. 267, 2018.

[3] S. G. Priori *et al.*, "HRS/EHRA/APHRS expert consensus statement on the diagnosis and management of patients with inherited primary arrhythmia syndromes," *J. Arrhythmia*, vol. 30, no. 1, pp. 1–28, 2014.

[4] J. Schläpfer and H. J. Wellens, "Computer-interpreted electrocardiograms: benefits and limitations," *J. Am. Coll. Cardiol.*, vol. 70, no. 9, pp. 1183–1192, 2017.

[5] J. An, Z. Li, D. J. Dzikowicz, B. Bailey, and M. Silka, "Brugada Detection from 12-Lead ECG Using a Multi-Scale Hybrid Transformer with Explainability," in *2026 Computing in Cardiology (CinC)*, 2026, pp. 1–4.

[6] C. Cortez *et al.*, "Brugada-HUCA: 12-Lead ECG Recordings for the Study of Brugada Syndrome," *PhysioNet*, 2026.

Address for correspondence:

Junmo An, PhD
222 Jacobs St,
Cambridge, MA 02141, USA
junmo.an@philips.com